**Noname manuscript No.**
(will be inserted by the editor)

# Image stylization using anisotropic reaction diffusion

**Ming-Te Chi · Wei-Ching Liu**

Received: date / Accepted: date

**Abstract** Image stylization refers to a process to convert photo-realistic images into a novel representation that express the content via particularly designed patterns. The fundamental steps to create different stylization lie in designing new patterns and creating an appropriate distribution. However, such task is mastered only by skilled artists and is challenging for most user. In this paper, we propose a novel image stylization system based on anisotropic reaction diffusion to facilitate the generation of pattern and image rendering. The system starts by generating various self-organized patterns using a modified reaction diffusion formulae. To enable more effective control over pattern generation, the proposed method involves using a set of modifications of anisotropic diffusion to control shape and introduces a flow field to guide pattern arrangement. In postprocess, we introduce new thresholding and color mapping method in postprocess to refine the size, density, and color of pattern . We demonstrate the effectiveness of our system using a large number results, showing that with a proper control on the parameters our system is able to generate versatile stylizations including paper-cut, stylized halftone image, and motion illusion.

**Keywords** image stylization · reaction diffusion · pattern generation

## 1 Introduction

The rapid development of digital authoring tool has expanded in scope to the creation of artworks featuring new styles. An easily controllable and diversified authoring tool can improve efficiency and facilitate creativity among artists. Image stylization is an essential nonphotorealistic rendering (NPR) technique that can be used to modify the style of input images, enhance image features, and express visual cues. It can be defined as a form of pattern generation that involves shapes and distributions. Pattern generation has been widely adopted in texture synthesis and decoration design.

Biological patterns, such as leopard spots and zebra stripes, can be generated using reaction diffusion. Reaction-diffusion systems are mathematical models that are used to describe the interaction of multiple chemicals. Many studies [10,15–17] have applied reaction diffusion to generate patterns. Although reaction diffusion can be used to generate complex patterns by simple formulae, the method offers poor control over detail. The core concept of the proposed system involves guiding the reaction-diffusion system along the flow direction to produce a stylized pattern distribution that conforms to the features of the input image. Using anisotropic diffusion enables us to adjust patterns easily by applying only a few parameters.

In this study, the proposed system was applied to yield images in the paper-cut, stylized halftone, and flow visualization styles. To create quality images that depict salient features, all of these patterns require distinct primitive placements and the use of geometric shapes. The paper-cut style can be considered a collage of geometric patterns, and the image in the paper-cut style was created using a binary thresholding process. By contrast, in the stylized halftone style, continuous tones are depicted by arranging smaller primitives by size, shape, and distribution. Because of the variety of primitives, recreated images are vivid and expressive. In addition, flow is another essential image character-

Ming-Te Chi
National Chengchi University.
E-mail: mtchi@cs.nccu.edu.tw

Wei-Ching Liu
National Chengchi University.

istic. Determining how to place stylized primitives to depict flow is crucial in flow visualization and image stylization. Furthermore, flexible control was required to produce the stylizations in this study to ensure that pattern generation yielded compelling results. The proposed method was applied, and the results confirmed that the method satisfied these requirements.

The main contributions of the proposed method are:

- It extends the existing reaction diffusion model by using anisotropy and flow fields, and provides flexible control of pattern generation for various applications. The method favorably preserves the tone and flow features of the input image based on the control image and flow field.
- It transfers the density field of the reaction diffusion into a stylized pattern by using the tone-preserving thresholding method.
- It converts the results of reaction diffusion by using polar angle parameterization and color mapping to create flow visualization featuring illusory motion.

In Section 2, previous studies related to this approach pertaining to reaction diffusion and flow-based image stylizations are reviewed. Section 3 describes the main framework for anisotropic reaction diffusion, including the basic concepts of reaction diffusion and ways to modify anisotropic diffusion to control stylization appropriately. In Section 4 the capabilities of this approach are demonstrated by presenting the results of applying the approach to create images in the paper-cut, stylized halftone, and flow visualization styles. In Section 5, the conclusion, the strengths and limitations of this approach are considered and future research directions are discussed.

## 2 Related work

### 2.1 Reaction diffusion

In 1952, Alan Turing proposed the reaction diffusion system [15], which describes the reaction of two chemical substances in morphogens. The reaction diffusion equation can be used to generate biological patterns, which is why numerous studies on pattern generation and texture synthesis have been inspired by the reaction diffusion system. Witkin and Kass [17] and Turk [16] have applied the reaction diffusion system to surface texture, generating various types of spot and stripe pattern. The additional anisotropic diffusion term extended the range of patterns and enabled control over resulting patterns. However, controlling patterns to generate specific shapes has remained difficult. Not only biological patterns have been produced: McGraw [10] introduced the tensor to represent high-order diffusion displacement in order to generate inorganic patterns.

Few approaches have addressed reaction diffusion by using flow fields. Sanderson et al. [13] proposed an adjusted anisotropic diffusion for deformed spot patterns to visualize a flow field. Kim and Lin [6] introduced an anisotropy-embedding function and an advection term to expand the range of patterns. We extended this approach to implement anisotropic designs in a flow field to enhance shaping and color mapping in order to provide more effective flow visualization.

### 2.2 Image stylization

Numerous researchers have attempted to implement the principles and techniques of various kinds of art in computer graphics. Xu et al. [19] presented a paper-cut style generated from bitonal images under geometric connectivity constraints. Xu et al. [18] introduced a novel concept to depict continuous-tone images by applying optimized thresholding to bitonal images while retaining salient features. This bitonal approach can also be used to control abstraction in image rendering.

Among the rich, diverse image stylization techniques that are available, flow-based stylization methods are reviewed here. Bousseau et al. proposed video watercolorization [2]: they adapted texture advection along the optical flow to maintain the coherence of the watercolor style. Kyprianidis et al. [7] and Kang et al. [5] have generated flow fields based on the edge tangent flow (ETF) from source images. Using the ETF enables strengthening the continuity of stylized lines and ensuring that stylized images are smoother, compared with traditional methods. Lee et al. [8] exploited the flow field to develop a texture-transfer method. The method by Li et al. [9] enables users to design geometric patterns by applying field-guided shape grammars. In addition to producing basic designs, resulting patterns can be ornamented with the flow field with minimal distortion. Son et al. proposed a stippling algorithm [14] that can effectively maintain the dot distribution in the application of the flow field, and this method can be used to reproduce the tones and features of input images.

### 2.3 Flow field

Generating a flow field to reflect the salient features of the input image was key to preserving visual cues in our study. To automatically generate the flow field from the input image, Kang et al. [4] proposed a flow-generating method that involves transferring the gradients of the input image to flow vectors and drawing coherent lines

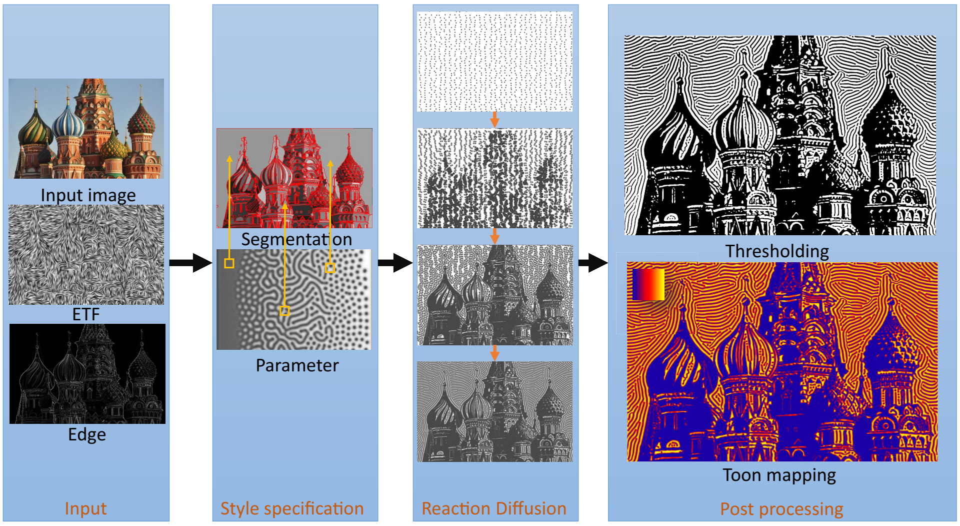


**Fig. 1** Flow chart of the proposed system.

by using the flow-based difference of the Gaussian filter. By segmenting the input image into subregions, Yao et al. [20] proposed an intuitive flow-design system that entails specifying simple operators for the partitions of the input image; their approach adapted harmonic functions to reduce singularity points on the flow field in order to express the topological structure of the partitions.

## 3 Method

To enable effective control over the patterns generated by reaction diffusion, the shape and pattern arrangement for anisotropic reaction diffusion were considered. Few studies have investigated anisotropic reaction diffusion. However, the generation of shapes and designs requires the fine adjustment of parameters. Furthermore, the flow field must be considered to ensure that pattern distribution reflects the feature of flow. The edge tangent flow (ETF) proposed by Kang et al. [4] was applied to generate flow fields comprising the salient features of the input image. Finally, the resulting density field from reaction diffusion process was converted into desired patterns by using thresholding or color mapping.

As shown in Figure 1, the process included the following main steps:

- The input image is converted into a flow field either by using the ETF or manually, according to the user's requirements.
- A control image is generated based on the salient features of the input image and user-specific parameters in order to guide the shape of the resulting reaction diffusion.
- Reaction diffusion is initialized using the input image, control image, and flow field. Multiple iterations are executed to automatically generate a stylized pattern. Iterations are conducted until the pattern is complete.
- Finally, the generated image is converted by using thresholding and color mapping to achieve a variety of artistic styles.

### 3.1 Reaction diffusion

A basic reaction-diffusion system takes the general form

$$\begin{aligned} \frac{\partial A}{\partial t} &= D_A \nabla^2 A + R_A(A,B) \\ \frac{\partial B}{\partial t} &= D_B \nabla^2 B + R_B(A,B) \end{aligned} \tag{1}$$

where $A$ and $B$ denote the density field of two chemicals. The equation describes the change in density field of $A$ and $B$ over time. The first term is the diffusion term, $D_A$ and $D_B$ denote the diffusion rate, and $\nabla^2 A$ is the Laplacian of $A$. The second term, $R_A(A,B)$, is the function that describes the reaction. The Gray-Scott model is one of the common models for reaction diffusion and is given by

$$\begin{aligned} &D_A : D_B = 2:1 \\ &R_A(A,B) = -AB^2 + F(1-A) \\ &R_B(A,B) = AB^2 - (F+k)B \end{aligned} \tag{2}$$

In the diffusion term, the diffusion rate of $A$ is two times faster than that of $B$. For the reaction term, the equation shows that one unit of $A$ and two units of $B$ will become to three units of $B$. $F$ and $k$ are parameters specified by the user to control the replenishment rate of $A$ and the diminishment rate of $B$. $(F+k)$ is used to guarantee the decreasing speed of $B$, which is faster than the production speed of $A$.

## 3.2 Pattern type and control function

The relationship between pattern styles and the reaction diffusion model was studied by Pearson [11]. He illustrated the parameterizations of the Gray-Scott model and classified the patterns into several types; Figure 2 shows the pattern types and the parameter spaces of the Gray-Scott model. The proposed method, by introducing the control function, applied these stable and stylized types of pattern to yield a great variety of stylization.

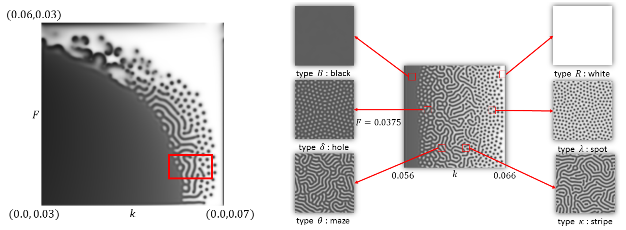


(a) (b)

**Fig. 2** Parameterizations in the Gray-Scott model. (a) shows the different pattern types in $F$ and $k$; stable pattern types in the red area are shown in (b), and were classified by Pearson [11].

In the following subsection, we consider three main control factors – scale, deformation, and rotation – in pattern generation.

### 3.2.1 Scaling factor

To generate a scalable pattern, one common approach is to adjust the speed rate of the diffusion and reaction terms to control the size of the generated pattern:

$$\frac{\partial A}{\partial t} = S_D D_A(\nabla^2 A) + S_R(R_A(A,B))$$
$$\frac{\partial B}{\partial t} = S_D D_B(\nabla^2 B) + S_R(R_B(A,B)) \qquad (3)$$
$$0 < S_D, S_R \leq 1$$

where $S_D$ and $S_R$ are the speed rate of the diffusion and reaction terms, respectively, and $S_D/S_R$ is proportional to the pattern size; the parameter space of $S_D$ and $S_R$ is shown in Figure 3. We set $S_D$ and $S_R$ greater than 0 to avoid generating failure patterns.

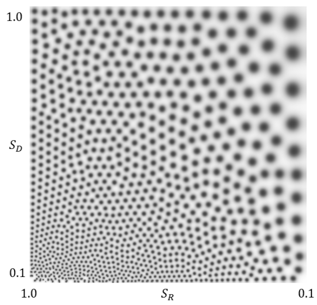


**Fig. 3** Parameter space of $S_D$ and $S_R$.

### 3.2.2 Anisotropic diffusion

Pattern deformation should be adjustable through anisotropic diffusion to enable flexible control in reaction diffusion systems. We applied the anisotropic diffusion term as

$$\frac{\partial A}{\partial t} = D_A(\nabla \cdot a(\theta(V, \nabla A))\nabla A) + R_A(A,B)$$
$$\frac{\partial B}{\partial t} = D_B(\nabla \cdot a(\theta(V, \nabla B))\nabla B) + R_B(A,B) \qquad (4)$$

where $a()$ denotes the anisotropic function, and $\theta(V, \nabla A)$ denotes the angle between the flow field $V$ and the gradient field of $A$. The generated pattern is then deformed according to the anisotropic function and flow field. For example, a spot pattern is deformed to a spindle pattern in Figure 7(b), and the pattern orientation follows the flow field.

According to the Gray-Scott model, the diffusion rates $D_A$ and $D_B$ are generally set at 2:1 in isotropic diffusion. Using Eq. 3 can ensure that the spot pattern, generated by ($F = 0.0300$, $k = 0.0655$), is stable and regular in isotropic diffusion. However, this rule is broken when the anisotropic diffusion is not a symmetric polar function. For example, with an anisotropic function specified as $a(\theta) = sin(0.5\theta)$, the patterns are unstable and keep changing in anisotropic diffusion when various angles ($\theta(V, \nabla A)$ for $A$, $\theta(V, \nabla B)$ for B) are used, as shown in Figure 4. Thus, we modified the anisotropic diffusion to ensure that the patterns would deform anisotropically but maintain stability as in isotropic diffusion. The modified formula is

$$\frac{\partial A}{\partial t} = D_A(\nabla \cdot a(\theta(V, \nabla B))\nabla A) + R_A(A,B)$$
$$\frac{\partial B}{\partial t} = D_B(\nabla \cdot a(\theta(V, \nabla B))\nabla B) + R_B(A,B) \qquad (5)$$

According to the modified formula, we maintained the diffusion rate at 2:1, as the anisotropic functions are the same for each element. We thus obtained the stable anisotropic pattern shown in Figure 4(b).

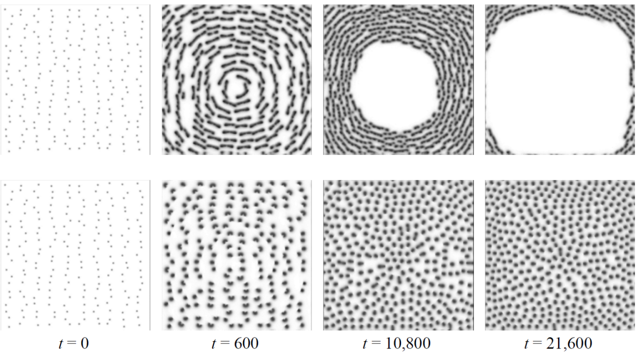


**Fig. 4** Comparison of stability in anisotropic diffusion. $t$ is iteration times. Top row: The resulting pattern is unstable when nonsymmetrical anisotropic diffusion is used . Bottom row: The resulting pattern is stabilized by applying the modified anisotropic diffusion. We use $F$=0.0300 and $k$=0.0655 (type $\lambda$: spot-like pattern) in both cases.

Kim and Lin [6] proposed the following diffusion term in discretized form:

$$\nabla \cdot a(\theta)\nabla A \approx \frac{1}{D_{\eta(i)}} \sum_{j\in\eta(i)} \frac{1}{||x_j - x_i||} \frac{a(\theta_i) - a(\theta_j)}{2} (A_j - A_i)$$
$$a(\theta) = \frac{m}{2}(1 + cos(l(\theta + \theta_0)),$$
$$m = a_n,\ when \frac{(n-2)\pi}{l} < (\theta + \theta_0) \le \frac{n\pi}{l} \tag{6}$$

The effect of the distance to neighbor is reduced because the distance $||x_j - x_i||$ is inversely proportional to the diffusion weight, and $D_{\eta(i)}$ is the sum of the distance. The function $a(\theta)$ in Eq. 6 is a general cosine-based anisotropy function where $\theta_0$ denotes the rotation angle and $l$ controls the edge number of the generated polygon pattern; the user can control both parameters. Figure 5 shows various parameters and their resulting patterns. The flow field $V$ in these results contains outward flow from center. The detailed parameters can be found in Table 1.

In addition, the user can also modify the anisotropic function. For example, user can specify different anisotropic function to each portion. For example, Eq. 7 demonstrate an unsymmetrical pattern by setting the part in 0 $\sim$ 180 degree to a constant. The waterdrop and sector patterns can be generated by the modified anisotropic functions in Figure 6.

$$a(\theta) = \begin{cases} 1, & if\ 0 \le (\theta + \theta_0) \le \pi, \\ \frac{m}{2}(1 + cos(l(\theta + \theta_0)), & otherwise. \end{cases} \tag{7}$$

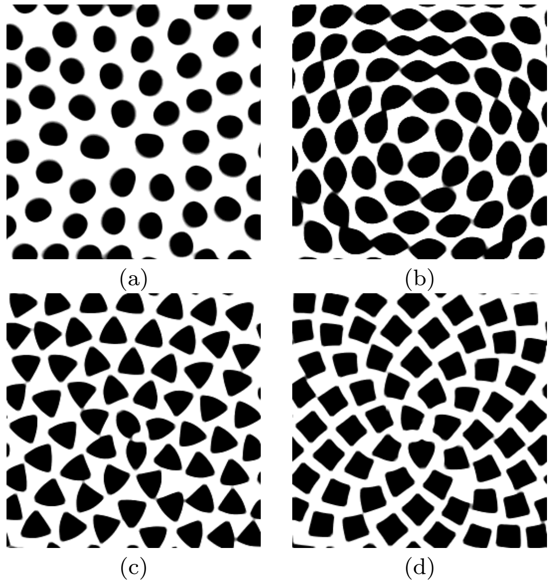


**Fig. 5** Spot patterns generated by the cosine-based anisotropy function in Eq. 6; $l$=1, 2, 3, 4 in (a) to (d).

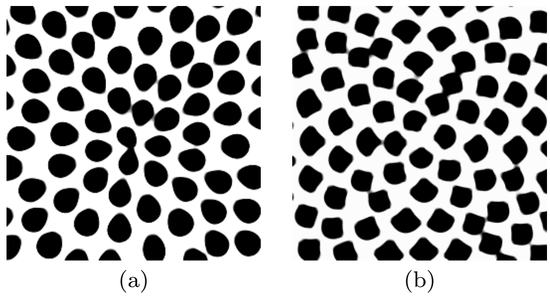


**Fig. 6** Stylized spot patterns generated by Eq. 7; (a) water drop, and (b) sector.

**Table 1** Pattern style and control parameters.

| Style | $a(\theta)$ | $F$ | $k$ | $l$ | Figure |
|---|---|---|---|---|---|
| semicircle | Eq. 6 | .0375 | .0655 | 1 | Fig. 5(a) |
| spot: spidle | Eq. 6 | .0375 | .0655 | 2 | Fig. 5(b) |
| hole: spidle | Eq. 6 | .0300 | .0546 | 2 | Fig. 8 blue |
| stripe | Eq. 6 | .0300 | .0620 | 2 | Fig. 8 green |
| triangle | Eq. 6 | .0375 | .0655 | 3 | Fig. 5(c) |
| spot: quad | Eq. 6 | .0375 | .0655 | 4 | Fig. 5(d) |
| water drop | Eq. 7 | .0375 | .0655 | 2 | Fig. 6(a) |
| sector | Eq. 7 | .0375 | .0655 | 4 | Fig. 6(b) |

### *3.2.3 Flow-guided diffusion*

In the previous section, patterns were deformed using the anisotropic function. However, this function had some limitations. Figure 7(b) shows the spindle spot. Each spot is deformed by an anisotropic function by using the flow field. However, each spot maintains an equal distance to neighboring spots because of the fixed and regular Laplacian kernel specified in Eq. 6. We adopted flow-guided diffusion in our system to correlate the arrangement to the flow field. A flow-guided diffusion is presented, in which the Laplacian kernel – rather than a regular kernel, as shown in Figure 7(a) – is deformed along the flow field, as shown in Figure 7(c). Flow-guided diffusion can be considered an arrangement factor in pattern control. In Figure 7(d), the patterns in flow-guided diffusion are arranged with the flow field but differ from those from regular kernels, thus deforming the shape of the pattern.

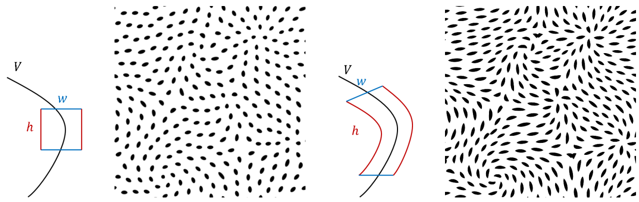


**Fig. 7** Comparison of different diffusion terms. (a) Fixed diffusion kernel, (b) Anisotropic diffusion, (c) Flow-guided diffusion kernel, and (d) Flow-guided anisotropic diffusion.

*3.2.4 Control parameters*

For image stylization, we segmented the input image into several subregions. Each subregion had distinct control parameters for the equations presented previously. The flow field can be generated from the input image by using the ETF [5]; subsequently, the pattern deformation and arrangement can be controlled by modifying the flow field. The pattern style can be controlled by modifying $F$ and $k$ in the Gray-Scott model, and pattern size can be controlled by modifying $S_D$ and $S_R$. In Figure 8, the control image and pattern styles are mapped; the control image can be generated based on the tone of the input image or designed manually.

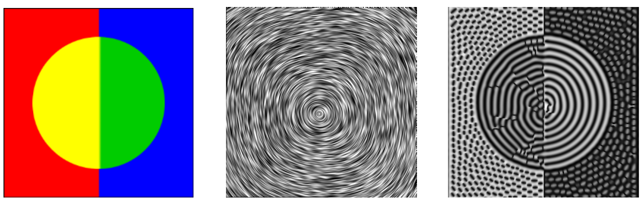


**Fig. 8** Pattern styles controlled using the control image and flow field. (a) control image; each region was accorded different parameters. Red: spot, blue: hole, green: line and yellow: inverse line. (b) flow field, (c) generated density field.

## 3.3 Post process

*3.3.1 Tone preserving thresholding*

When generating a reaction-diffusion pattern, the resulting density field is generally blurred, and the contour is soft because of the nature of the diffusion process. Figure 9 shows the process from the density field to black/white patterns. First, the adaptive histogram equalization [12] was applied to the density field to ensure that the local maximum was consistent. Second, thresholding was used to segment the density field into patterns with clear shapes. However, the size of the pattern affected by a global thresholding value may not reflect the tones in the input image. To produce a tone-preserving pattern automatically, we split the histogram of the input image into several bins with equal size to compute appropriate thresholding values for each gray value. Each pixel in the density field was locally thresholded to black/white according to the thresholding values of the tone image, such that the pattern size was adjusted to match the tone map. Figure 10 shows how tone-preserving thresholding can be used to transform the density field into patterns of a similar tone to the input image.

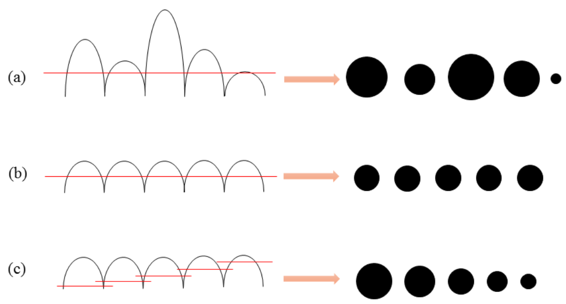


**Fig. 9** Different thresholding processes. The left column shows a 2D profile of the density field. The right column shows the thresholded patterns from the left. (a) Each pattern may not have been evenly distributed in the density field, and the global thresholding patterns were nonuniform. (b) By modifying the distribution of the density field, the thresholding pattern was made uniform; subsequently, (c) multiple thresholding values were used to render the pattern in different sizes.

*3.3.2 Direction preserving color mapping*

Although desired patterns may be generated using parameter adjustment and thresholding, a single-channel density field in reaction diffusion limits color presentation. The generated destiny field can only be converted into a gray image. Thus, to express more information, such as the direction, magnitude of the flow field, and

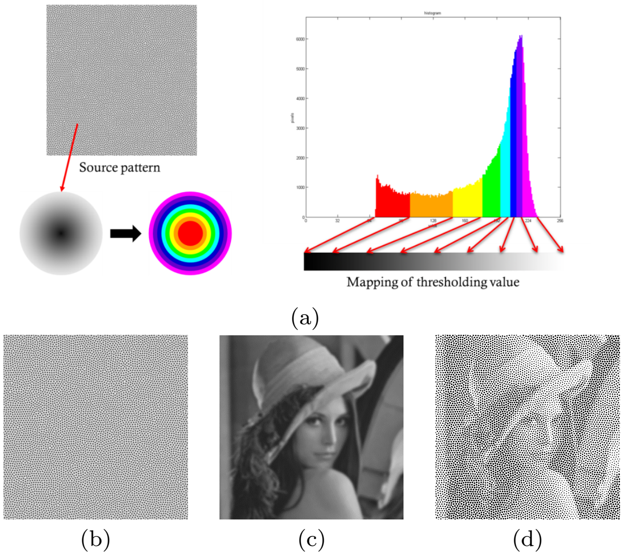


**Fig. 10** Thresholding process. A tone image (c) was mapped to several appropriate thresholding values by using clipping histograms; the density field (b) was transformed to a halftone result (d).

color of the input image, we referred to the work of Barla et al. [1] regarding extended toon-shading. They used a 2D texture map to encode both shading and viewing distance information for various shading effects. We adapted this multi-parameter information on a 2D map. Additionally, the 2D color mapping method provides flexibility in visual effects.

In reaction diffusion, the pattern grow from center. We try to parameterize the pattern space into polar angle coordinate. In our observation, the density value of pattern center is a local maximum. Thus, the diffuse direction of the density field in the reaction diffusion can be expressed by the gradient of density field. We considered the distance from $p_i$ to the center of the pattern to be the density value, and the angle between the flow direction $v_f^i$ and gradient of density field $v_g^i$, as shown in Figure 11(c). The polar coordinate conversion for each pixel $p_i$ is then given by

$$\begin{aligned} r_i &= A(p_i) \\ \theta_i &= cos^{-1}(\frac{v_g^i \cdot v_f^i}{|v_g^i||v_f^i|}) \end{aligned} \tag{8}$$

where $[r_i, \theta_i]$ denotes the radius and angle in the polar coordinate, and $v_f^i$ and $v_g^i$ denote the gradient vector of density field and direction vector of flow field for each pixel $p_i$, respectively.

The proposed polar coordinate representation is useful to visualize flow directions. We can extend it with motion illusion. Motion illusions are still images that contain special patterns for expressing the effect of motion. Chi et al. [3] proposed a color mapping method for mapping shading colors to repeated asymmetric patterns (a special color combination that can evoke motion illusion). Based on this concept, we encoded the repeated asymmetric pattern as polar coordinates, as shown in Figure 11(a). We divided the polar coordinates into three main regions according to radius: high-, middle-, and low-density. The high-density region was the pattern whereas the low-density region was the background. The middle region was separated into two subregions according to the angle. Figures 11(b) and (c) show the density field converted into a still image with motion illusion to depict a flow direction with Eq. 9; $C_i$ is the color of pixel $i$ and $r_{min}$ and $r_{max}$ are the range of the middle part.

$$C_i = \begin{cases} yellow & \text{if } r_{max} < r_i < \infty \\ black & \text{if } r_{min} < r_i < r_{max} \; and \; 0 < \theta_i < \pi \\ white & \text{if } r_{min} < r_i < r_{max} \; and \; \pi < \theta_i < 2\pi \\ blue & \text{if } 0 < r_i < r_{min} \end{cases} \tag{9}$$

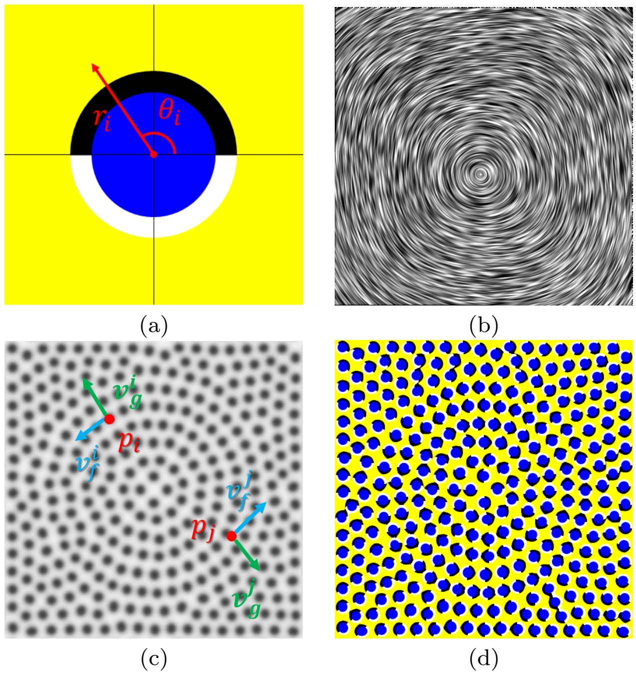


**Fig. 11** Motion illusion can be generated by color mapping. (a) Color map in polar coordinates, (b) flow field, (c) density field from reaction diffusion; (d) shows the results of the color mapping in (c).

## 4 Results

The proposed method was implemented using C++ and OpenCV. All experiments were evaluated on a PC with

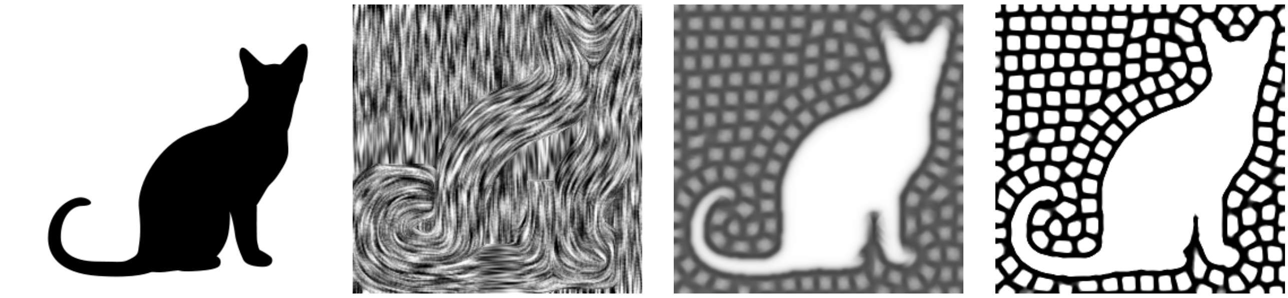


**Fig. 12** Simple paper-cut images. (a) Input image, (b) flow field, (c) generated pattern and (d) result with thresholding.

a 3.4GHz CPU and nVidia geforce GTX 670. The main cost of reaction diffusion involved the modified diffusion term, which is an iterative process with complex computation. However, it is suitable for parallel computation, our GPU implementation was faster than CPU as shown in Table 2. It taken 4 30 second to generated a stable result at most 50,000 iterations, and the resolution of the image did not affect iteration times. We tested various patterns to compare them with existing art works and to demonstrate the feasibility of the proposed method.

**Table 2** Performance.

| Resolution | FPS (CPU) | FPS (GPU) | Time |
|---|---|---|---|
| 256×256 | 62 | 2,210 | 4.5s |
| 512×512 | 18 | 1,311 | 7.6s |
| 1024×1024 | 4 | 323 | 30.9s |

### 4.1 Paper-cut art

Paper-cut art, comprising the repetition of patterns with clearly arranged shapes along the flow field, is a type of image stylization. In Myriam Dion's paper-cut art, images from newspapers are taken as the input; the flow direction is visualized by hollowing image using directional and closely arranged patterns. In our system, the direction and arrangement of the patterns can be controlled by modifying the flow field. By generating a black-and-white pattern, the user can create images in the paper-cut style. Figure 12 shows a simple case of paper-cut art with a quad pattern arrangement in the flow field. Starry night demonstrates a complex paper-cut in Figure 13, we used flow-guided spindle patterns to replace the sky and distinguished the regions of clouds, stars and the moon by different arrangement and deformed parameters. Figure 14 demonstrates another complex case with multiple stylized patterns: we enlarged the size of the pattern from the center to the border to enhance the visual effects of the blooming flowers.

### 4.2 Styled halftone images

We also created images in the stylized halftone style. In Marcos Marin's stylized halftone artwork, in which portrait photographs are taken as the input images, and line-type patterns were used to replace the input image. To express the luminance of the input image, the thickness of line patterns was mapped by the level of luminance; thus, the completed artworks are stylized halftone images or optical artworks. We used thresholding control to transform the anisotropic spot pattern into a stylized halftone image, as shown in Figure 15. A more complex case of the stylized halftone style with optical art effects is shown in Figure 16. In addition to the single-pattern style, our system also enables multiple patterns to be specified in segmented images. For segmented images, we assigned different parameters to each region to generate multiple patterns in the image shown in Figure 17.

### 4.3 Flow-field visualization

In addition to image stylization, our method enables flow visualization. To visualize flow-field information, we specified control factors in regard to the orientation and magnitude of the flow field. Patterns deformed by anisotropic diffusion can indicate the orientation of the flow field, and the pattern size can provide an intuitive map to the magnitude. In our results, shown in Figure 18, the magnitude of the flow field was indicated by the deformed circle along the flow direction. Compared with the results of Sanderson et al. [13], the proposed color mapping method facilitated generating the motion illusion effect. Figure 19 shows an alternative color mapping method used to convert the density field into a quad/triangle pattern; because reaction diffusion

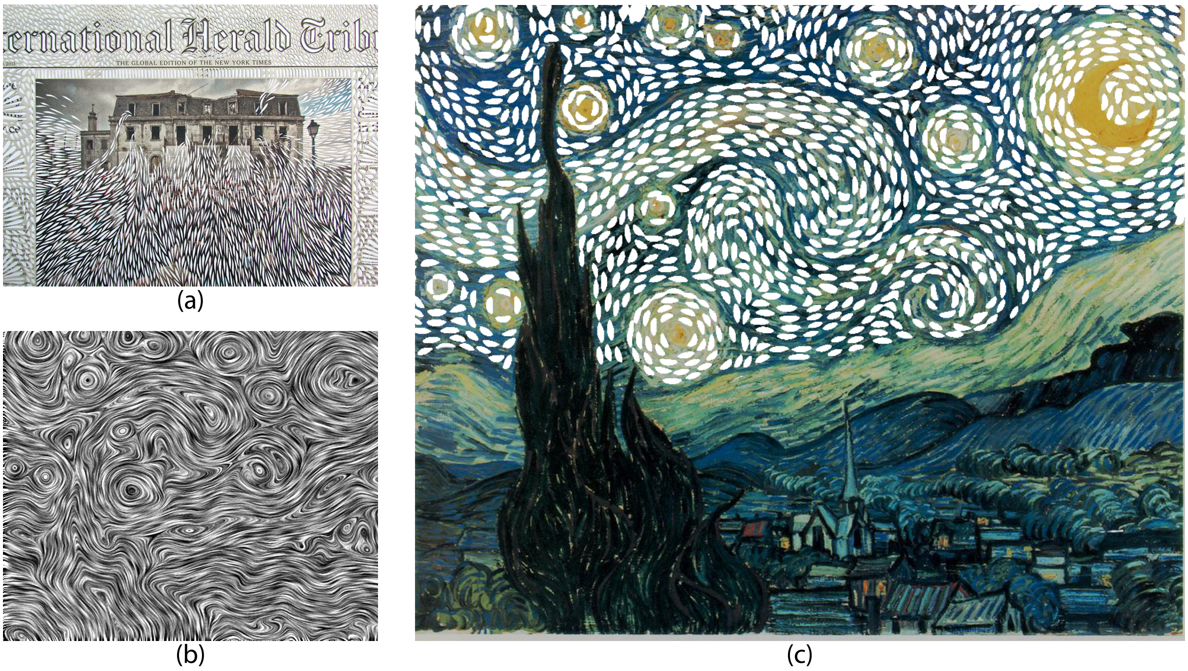


**Fig. 13** Complex paper-cut images. (a) Paper-cut art by Myriam Dion, (b) flow field, and (c) a recreated Starry Night by using the proposed method.

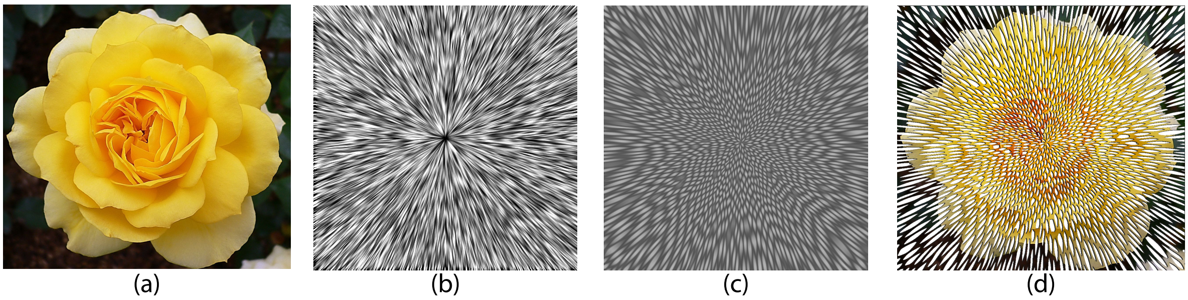


**Fig. 14** Complex paper-cut art. (a) Source image, (a) Flow field, (c) density field generated by reaction diffusion, and (d) result.

is self-organizing, a favorable pattern distribution was obtained automatically.

## 5 Conclusions

This study proposes an anisotropic pattern generation method for image stylization. The method integrates flow fields and controllable reaction diffusion. The core algorithm was created by extending the reaction diffusion model; the proposed method offers flexible control and maps complex parameters to common stylized patterns. Consequently, it can be used to produce images in various styles. In addition, thresholding and color mapping are proposed as optimal methods to be used in concert with the flow field and density distribution. The self-organizing properties of reaction diffusion permit a less regular pattern, thus, the results resemble handmade images. The effectiveness of the proposed system was confirmed by applying the system to create images in the paper-cut and stylized halftone styles.

In the future, the authors intend to extend the proposed method to include surface and volume data; however, this requires to meet the challenge of redefining the anisotropic Laplacian kernel on the 3D domain and reducing the costs of complex computation. Furthermore, the method may be integrated with additional reaction diffusion models and extended to produce a greater variety of patterns. The system has certain limitations. For example, when the flow field was discontinuous, the generated patterns become noisy and broken. Moreover, because the generated patterns were obtained by deforming patterns resulting from reaction diffusion, the method may have certain natural limita-

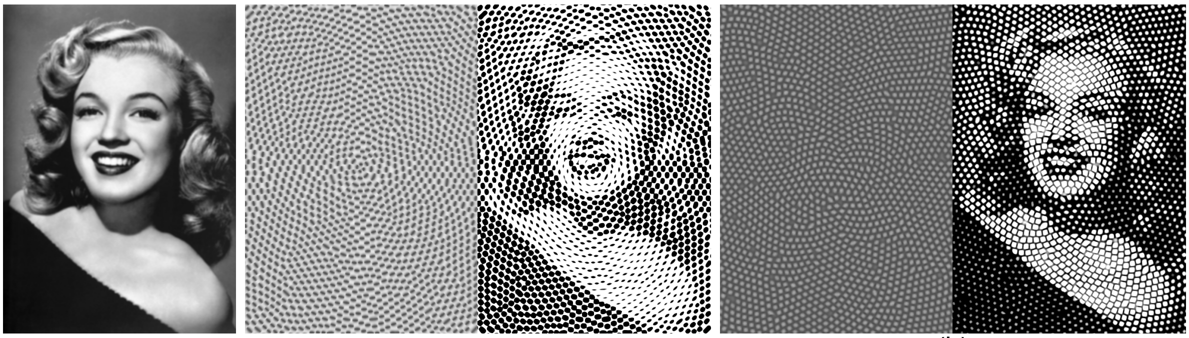


**Fig. 15** Halftone image with thresholding control. Control image control the thresholding value. Spindle spot pattern (a) and quad hole pattern (b) are used with vortex flow field.

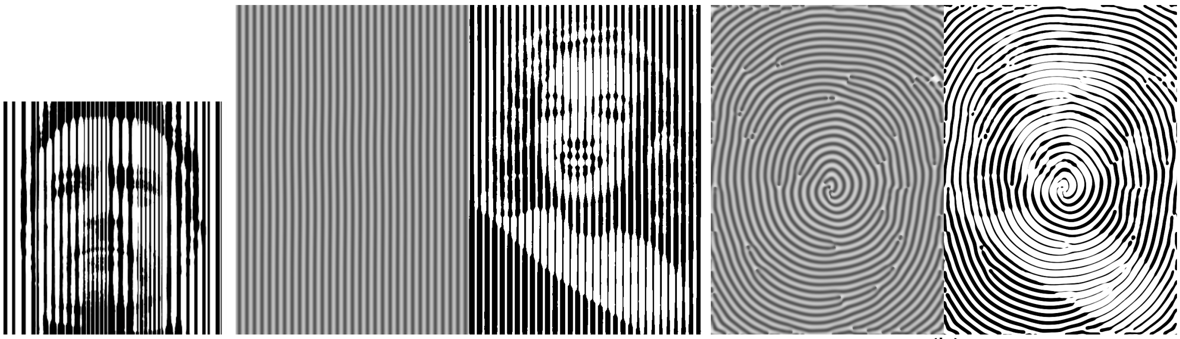


**Fig. 16** Stylized halftone images inspired by Marcos Marin's art. Stripe patterns were used with straight (a) and vortex (b) flow fields.

tions in generating certain complex patterns, for example, snowflake patterns.

**Acknowledgements** We would like to thank the anonymous reviewers and the editor for their valuable comments. This work is supported by the ministry of science and technology, Taiwan under MOST 103-2221-E-004-008.

## References

1. Barla, P., Thollot, J., Markosian, L.: X-toon: An extended toon shader. In: Proceedings of the 4th International Symposium on Non-photorealistic Animation and Rendering, NPAR '06, pp. 127–132. ACM, New York, NY, USA (2006)
2. Bousseau, A., Neyret, F., Thollot, J., Salesin, D.: Video watercolorization using bidirectional texture advection. In: ACM SIGGRAPH 2007 Papers, SIGGRAPH '07. ACM, New York, NY, USA (2007)
3. Chi, M.T., Lee, T.Y., Qu, Y., Wong, T.T.: Self-animating images: illusory motion using repeated asymmetric patterns. In: ACM Transactions on Graphics (TOG), vol. 27, p. 62. ACM
4. Kang, H., Lee, S., Chui, C.K.: Coherent line drawing. In: Proceedings of the 5th International Symposium on Non-photorealistic Animation and Rendering, NPAR '07, pp. 43–50. ACM, New York, NY, USA (2007)
5. Kang, H., Lee, S., Chui, C.K.: Flow-based image abstraction. IEEE Transactions on Visualization and Computer Graphics **15**(1), 62–76 (2009)
6. Kim, T., Lin, M.: Stable advection-reaction-diffusion with arbitrary anisotropy. Comput. Animat. Virtual Worlds **18**(4-5), 329–338 (2007)
7. Kyprianidis, J.E., Döllner, J.: Image abstraction by structure adaptive filtering. In: Proc. EG UK Theory and Practice of Computer Graphics, pp. 51–58 (2008)
8. Lee, H., Seo, S., Ryoo, S., Yoon, K.: Directional texture transfer. In: Proceedings of the 8th International Symposium on Non-Photorealistic Animation and Rendering, NPAR '10, pp. 43–48. ACM, New York, NY, USA (2010)
9. Li, Y., Bao, F., Zhang, E., Kobayashi, Y., Wonka, P.: Geometry synthesis on surfaces using field-guided shape grammars. Visualization and Computer Graphics, IEEE Transactions on **17**(2), 231–243 (2011)
10. McGraw, T.: Generalized reaction diffusion textures. Computers & Graphics **32**(1), 82–92 (2008)
11. Pearson, J.E.: Complex patterns in a simple system. Science **261**(5118), 189–192 (1993)
12. Pizer, S.M., Amburn, E.P., Austin, J.D., Cromartie, R., Geselowitz, A., Greer, T., Romeny, B.T.H., Zimmerman, J.B.: Adaptive histogram equalization and its variations. Comput. Vision Graph. Image Process. **39**(3), 355–368 (1987)
13. Sanderson, A.R., Johnson, C.R., Kirby, R.M.: Display of vector fields using a reaction-diffusion model. In: Proceedings of the Conference on Visualization '04, VIS '04, pp. 115–122. IEEE Computer Society, Washington, DC, USA (2004)

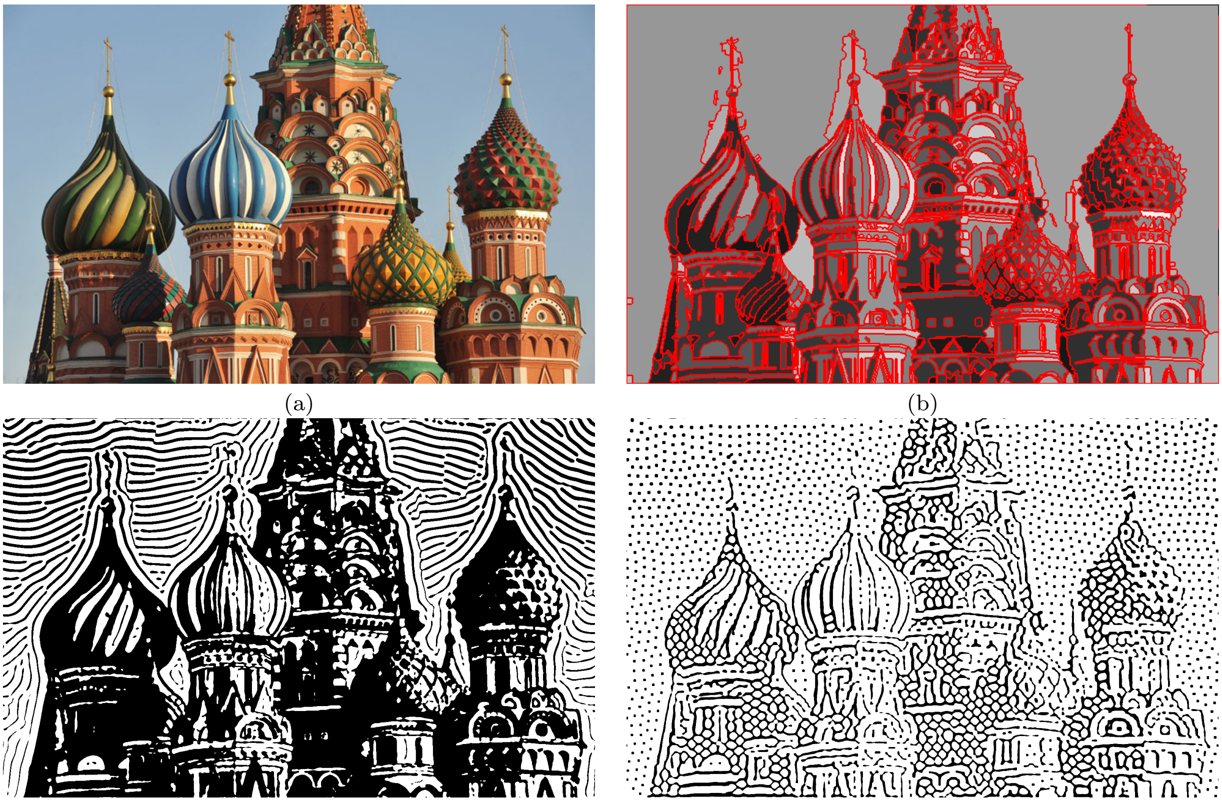

(a) (b) (c) (d)

**Fig. 17** Stylized halftone images featuring multiple patterns. The input image (a) was segmented into several regions (b). The user can assign different parameters to each region. (c) shows the use of black, white, and line pattern styles. (d) shows the use of quad-spot and hole pattern styles.

14. Son, M., Lee, Y., Kang, H., Lee, S.: Structure grid for directional stippling. Graphical Models **73**(3), 74–87 (2011)
15. Turing, A.: The chemical basis of morphogenesis. Philosophical Transactions of the Royal Society of London. Series B, Biological Sciences **237**(641), 37–72 (1952)
16. Turk, G.: Generating textures on arbitrary surfaces using reaction-diffusion, vol. 25. ACM (1991)
17. Witkin, A., Kass, M.: Reaction-diffusion textures. ACM Siggraph Computer Graphics **25**(4), 299–308 (1991)
18. Xu, J., Kaplan, C.S.: Artistic thresholding. In: Proceedings of the 6th International Symposium on Non-photorealistic Animation and Rendering, NPAR '08, pp. 39–47. ACM, New York, NY, USA (2008)
19. Xu, J., Kaplan, C.S., Mi, X.: Computer-generated papercutting. In: Proceedings of the 15th Pacific Conference on Computer Graphics and Applications, PG '07, pp. 343–350. IEEE Computer Society, Washington, DC, USA (2007)
20. Yao, C.Y., Chi, M.T., Lee, T.Y., Ju, T.: Region-based line field design using harmonic functions. Visualization and Computer Graphics, IEEE Transactions on **18**(6), 902–913 (2012)

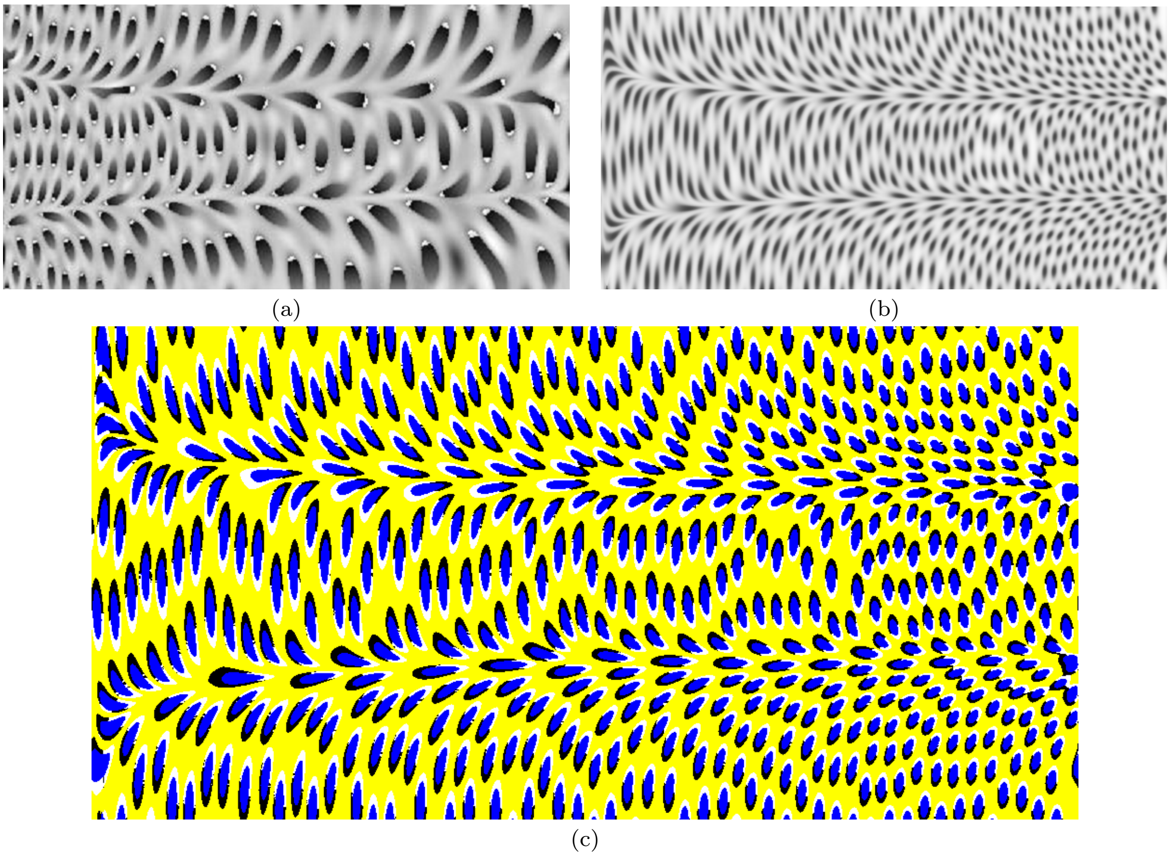


**Fig. 18** Flow visualization comparison. (a) is from Sanderson et al. [13]; our method is shown in (b), in which a density field generated by reaction diffusion is depicted; (c) shows motion illusion by using color mapping.

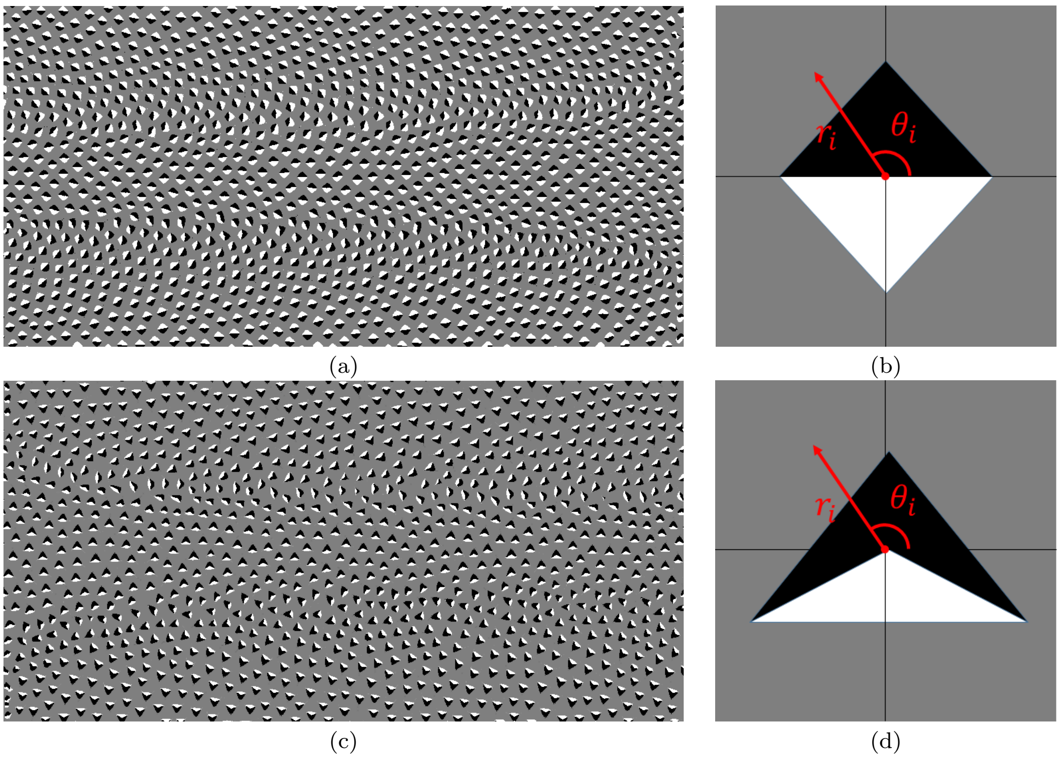


**Fig. 19** Flow visualization. Quad (a) and triangle (c) spot patterns were generated – black for the forward direction, white for backward direction, and grey for the background – by using the color mapping method shown in (b) and (d).